International Journal of Nanomedicine

Dovepress

open access to scientific and medical research

Open Access Full Text Article

ORIGINAL RESEARCH

Biocompatibility of Fe_3O_4@Au composite magnetic nanoparticles in vitro and in vivo

This article was published in the following Dove Press journal:
International Journal of Nanomedicine
8 November 2011
Number of times this article has been viewed

Yuntao Li[1,2]
Jing Liu[1]
Yuejiao Zhong[3]
Jia Zhang[1]
Ziyu Wang[1]
Li Wang[1]
Yanli An[1]
Mei Lin[1]
Zhiqiang Gao[2]
Dongsheng Zhang[1]

[1]School of Medicine, Southeast University, Nanjing, Jiangsu Province, People's Republic of China; [2]Second Affiliated Hospital of Nanjing Medical University, Nanjing, Jiangsu Province, People's Republic of China; [3]Jiangsu Cancer Hospital and Jiangsu Institute of Cancer Research, Nanjing, Jiangsu Province, People's Republic of China

Purpose: This research was conducted to assess the biocompatibility of the core–shell Fe_3O_4@Au composite magnetic nanoparticles (MNPs), which have potential application in tumor hyperthermia.

Methods: Fe_3O_4@Au composite MNPs with core–shell structure were synthesized by reduction of Au^{3+} in the presence of Fe_3O_4-MNPs prepared by improved co-precipitation. Cytotoxicity assay, hemolysis test, micronucleus (MN) assay, and detection of acute toxicity in mice and beagle dogs were then carried out.

Results: The result of cytotoxicity assay showed that the toxicity grade of this material on mouse fibroblast cell line (L-929) was classified as grade 1, which belongs to no cytotoxicity. Hemolysis rates showed 0.278%, 0.232%, and 0.197%, far less than 5%, after treatment with different concentrations of Fe_3O_4@Au composite MNPs. In the MN assay, there was no significant difference in MN formation rates between the experimental groups and negative control ($P > 0.05$), but there was a significant difference between the experimental groups and the positive control ($P < 0.05$). The median lethal dose of the Fe_3O_4@Au composite MNPs after intraperitoneal administration in mice was 8.39 g/kg, and the 95% confidence interval was 6.58–10.72 g/kg, suggesting that these nanoparticles have a wide safety margin. Acute toxicity testing in beagle dogs also showed no significant difference in body weight between the treatment groups at 1, 2, 3, and 4 weeks after liver injection and no behavioral changes. Furthermore, blood parameters, autopsy, and histopathological studies in the experimental group showed no significant difference compared with the control group.

Conclusion: The results indicate that Fe_3O_4@Au composite MNPs appear to be highly biocompatible and safe nanoparticles that are suitable for further application in tumor hyperthermia.

Keywords: toxicity, hyperthermia, core–shell

Introduction

In the past two decades, the development and implementation of innovative processes in the field of tumor hyperthermia were being extensively studied because of the innovation of biomedical nanomaterials. Many efforts have been made to design appropriate nanoparticles and nanocomposites for hyperthermia.[1,2] Based on the development of composite nanoparticles, core–shell superparamagnetic particles have attracted a broader interest because of their combined advantages of the heteromaterials. Among them, the applications of gold-coated iron oxide nanoparticles are of particular interest because they have not only the magnetism of iron oxide that renders them easily manipulated and heated by an external magnetic field, but also the excellent near-infrared (NIR) light sensitivity and strong adsorptive ability of the Au layer can

Correspondence: Dongsheng Zhang
School of Medicine, Southeast University, No. 87 Dingjiaqiao Road, Nanjing, Jiangsu Province 210009, People's Republic of China
Tel +86 25 8 327 2502
Fax +86 255 771 2900
Email zdszds1222@163.com

make them useful in photothermal therapy.[3–5] However, it should be noted that, while a considerable number of studies have been done on the synthesis and coating process of gold-coated iron oxide nanoparticles, attention devoted to the biocompatibility for in-vivo biomedical applications to ensure their safe clinical use of this kind of heteromaterial is still limited. The basic criteria for their clinical application are safety and good biocompatibility, which are also important to the industrialization of nanomedicine.[6,7]

The present authors' earlier research has shown that Fe_2O_3 and Fe_3O_4 magnetic nanoparticles (MNPs) achieve a satisfactory thermal therapeutic effect on cell lines and animal models of liver cancer and cervical cancer in magnetic fluid hyperthermia (MFH), without histological toxicity to nontarget organs or tissues.[8,9] Furthermore, in this present study highly crystalline, monodispersed core–shell multifunctional Fe_3O_4@Au composite MNPs were synthesized and used in MFH combined with NIR hyperthermia. The formation of the core–shell structure was achieved in two consecutive steps, seeding the Fe_3O_4 core followed by coating the gold shell. Well engineered Fe_3O_4@Au composite MNPs tend to accumulate in the tumor due to the unorganized nature of malignancy vasculature when they are injected into an organ with a tumor, and they have strong responsiveness and low heating effect under alternating magnetic field and NIR laser exposure, which can effectively guide heat to the tumor without damaging the normal tissue.[5] Although gold is an inert metal, the effect on normal cell proliferation cannot be underestimated. Moreover, the nature of the composite nanoparticles could remarkably affect their biocompatibility. Thus, the toxicity and biocompatibility of the complex in vitro and in vivo need to be thoroughly evaluated before the material can be applied in hyperthermia research.[10] Therefore, the cytotoxicity assay, hemolysis test, micronucleus (MN) assay, and detection of acute toxicity in mice and beagle dogs were introduced to evaluate the biocompatibility of self-assembled Fe_3O_4@Au composite MNPs in this research.[11,12]

Materials and methods

Main apparatus and reagents

The transmission electron microscope (TEM) used was an H-600 model (Hitachi, Tokyo, Japan), and the scanning electron microscope (SEM) was a JSM-6360 model (JEOL Ltd, Akishima, Japan). The energy dispersive spectrometer (EDS) was purchased from Thermo NORAN Vantage (Waltham, MA). The laser particle size analyzer and zeta potential analyzer were purchased from Malvern Instruments Ltd (Worcestershire, UK). A 752 prismatic ultraviolet-visible (UV-vis) spectrophotometer was purchased from Shanghai Precision Scientific Instrument Co, Ltd, (Shanghai, China). 3-(4,5-dimethylthiazol-2-yl)-2,5-diphenyltetrazolium bromide (MTT) and dimethyl sulfoxide were obtained from Sigma-Aldrich (St Louis, MO). RPMI-1640 medium was purchased from Gibco-Invitrogen Corp (Carlsbad, CA). Other reagents included ferric chloride, ferrous sulfate, and ammonia water (Hanguang Chemical Reagent Co, Ltd, Shanghai, China), $HAuCl_4$, NH_2OH_3HCl, and potassium oxalate (Shanghai First Reagent Factory, Shanghai, China), newborn calf serum (Si-Ji-Qing the Biotechnology Co, Ltd, Hangzhou, China), methanol (Zhenxing First Chemical Factory, Shanghai, China), cyclophosphamide (CTX) (Jiangsu Hengrui Medicine Co Ltd, Lianyungang, China), and Giemsa staining solution (Chroma, Bellows Falls, VT). All reagents were of analytical grade.

Cells and animals

Cell line L-929 was purchased from Shanghai Institute of Cell Biology (Shanghai, China). Kunming albino mice, age matched (6 weeks of age) and weight matched (18–22 g), New Zealand rabbits weight matched (2.5 kg), and beagle dogs, age matched (6–8 months of age) and weight matched (7–9 kg), were provided by the experimental animal center of Yangzhou University (Yangzhou, China). All animal experiments were evaluated and approved by the Animal and Ethics Review Committee of Southeast University (Nanjing, Jiangsu Province, China). All animals were maintained in a pathogen-free, air-conditioned environment at 24°C ± 2°C with a standard 12-hour light/12-hour dark cycle. The animals were allowed free access to tap water and food in the form of a standard pellet diet.

Preparation and characterization of Fe_3O_4@Au composite MNPs

Fe_3O_4-MNPs were prepared by the technique of chemical coprecipitation as previously published.[9] Fe_3O_4@Au core–shell composite nanoparticles were then synthesized by reduction of Au^{3+} in the presence of Fe_3O_4-MNPs, seeding the Fe_3O_4 core, followed by coating the gold shell. The operating procedure adopted was the following. First, the Fe_3O_4-MNP solution was diluted to 10 mM in deionized water, and 20 mL was stirred with 20 mL of 1 M sodium citrate for 10 minutes. Next, the solution was diluted with deionized water to 200 mL, and 1 mL of NH_2OH_3HCl solution of 1 M was added. Then, 1% $HAuCl_4$ (10 mL) was incrementally added dropwise with stirring. A total of three additions (each

for NH_2OH_3HCl and $HAuCl_4$) were performed during the reaction, and the stirring continued for at least 30 minutes after each addition. The clear black solution became brown at first addition and changed to garnet after three iterative additions. TEM and SEM were used to observe the morphological characteristics of Fe_3O_4@Au composite MNPs. Meanwhile, EDS was employed to assay their composition. A laser particle size analyzer and a zeta potential analyzer were used to detect their average diameter and zeta potential. In addition, the UV-vis spectra were acquired with a UV-vis spectrophotometer, and the magnetization was measured by a vibrating sample magnetometer integrated in a physical property measurement system (PPMS-9; Quantum Design, San Diego, CA) up to 5000 Oe at 300 K.

The cytotoxicity of Fe_3O_4@Au composite MNPs

MTT assay was used to evaluate cell toxicity.[13] The sterile nanoparticles were diffused at 100 mg/mL concentration in RPMI-1640 medium (containing 10% fetal calf serum) for 72 hours at 37°C. After centrifugation at 2500 rpm for 5 minutes, the supernatant was filtered to get leaching liquor of 100% concentration. L929 fibroblast cells were seeded in 96-well plates (6000 cells per well) for 24 hours in RPMI-1640 medium. Then they were divided into six groups (eight wells per group) and incubated with various concentrations of leaching liquor (100%, 75%, 50%, and 25% leaching liquor), RPMI-1640 medium containing 10% fetal calf serum (negative control) and 0.7% polyacrylamide (positive control) for 48 hours. Inverted microscopy was used to observe general morphological changes of the L929 cells, and then the MTT assay was performed and the optical density (OD) values were measured at 492 nm. The cell relative growth rate (RGR) was calculated as follows:

$$RGR = \frac{\text{OD of experimental group}}{\text{OD of negative control group}} \quad (1)$$

The toxicity grade is precise when the experimental results show grade 0 and grade 1. If the results show grade 2, the toxicity should be evaluated by both RGR and the morphological changes of cultured cells. The toxicity is uncertain when the results belong to other grades (Table 1).

Table 1 RGR and toxicity grade conversion

Toxicity grade	RGR
Grade 0	≥1
Grade 1	0.75–0.99
Grade 2	0.50–0.74
Grade 3	0.25–0.49
Grade 4	0.01–0.24
Grade 5	0

Abbreviation: RGR, relative growth rate.

Hemolysis test of Fe_3O_4@Au composite MNPs

Blood was obtained from healthy New Zealand rabbits and anticoagulated with potassium oxalate, at a final concentration of 1.0 mg/mL of blood. The Fe_3O_4@Au composite MNPs were rinsed three times with distilled water, lixiviated with 0.9% saline, with a final concentration reached of 100 mg/mL. 0.9% saline and distilled water were used as the negative control (0% hemolysis) and the positive control (100% hemolysis), respectively. The material detected was divided into three concentration groups, ie, 100, 75, and 50 mg/mL. Each group contained three test tubes, each of which contained either 10 mL leaching liquor of the material, 0.9% saline, or distilled water. Then, 0.2 mL of diluted anticoagulated blood was added to each tube preheated for 30 minutes at 37°C. After incubation for 60 minutes at 37°C, the tubes were centrifugated at 2500 rpm for 5 minutes. Next, the supernatant fluid was assembled, and OD values were measured at 545 nm by UV-vis spectrophotometry. The hemolysis rate (HR) was calculated using the mean OD value for each group as follows:

$$HR\ (\%) = (D_t - D_{nc})/(D_{pc} - D_{nc}) \times 100\%, \quad (2)$$

where D_t is the absorbance of the testing sample, and D_{pc} and D_{nc} are the absorbance of the positive control and the negative control, respectively.[14,15]

MN assay of Fe_3O_4@Au composite MNPs

The KunMing albino mice (20–22 g) were randomly divided into six groups; there were five females and five males in every group. The animals were then treated with 100 mg/mL Fe_3O_4@Au composite MNPs (5.00, 3.75, 2.50, and 1.25 g/kg), 0.9% saline (as negative group) and CTX 40 mg/kg (as positive group) respectively. All experimental mice were injected intraperitoneally twice, with a 24-hour interval, and then sacrificed 6 hours after the second administration. The thighbone marrows were extracted for smears, immobilized 5 minutes with methanol, and then stained with Giemsa for 15 minutes. At least 1000 polychromatic erythrocytes (PEC) were counted for each mouse, and the rate of formation of PEC containing MN was calculated.

Poisson distribution was used to analyze statistic difference between each group.[16]

Acute toxicity testing in mice

The KunMing albino mice were randomly assigned into eight groups, with five females and five males in each group. Fe_3O_4@Au composite MNPs dissolved in 0.9% saline with a concentration of 100 mg/mL were injected intraperitoneally into the mice at dosages of 1.77, 2.51, 3.54, 5.00, 7.06, 9.98, 14.09, and 19.89 g/kg. The general behavior of the mice was observed continuously for 1 hour immediately after injections and then intermittently observed for a period of 24 hours. All mice were further observed for up to 14 days after treatment, and general physical states, including respiration, eating, and movement were monitored. Any signs of toxicity and deaths were recorded. Median lethal dose (LD_{50}) was evaluated by the Karber method.[17] The animals were executed after the examination was finished.

Acute toxicity studies in beagle dogs

The animals were randomly divided into two groups: one experimental group and one control group, with three males and three females in each group. Normal parameters including body weight, temperature, appetite, and performance of the dogs were observed and recorded before Fe_3O_4@Au composite MNPs treatment. Fe_3O_4@Au composite MNPs dissolved in 0.9% saline with the concentration of 100 mg/mL were administered via liver injection at a dosage of 0.1 g/kg. The control group was injected with the same volume of 0.9% saline. The rate of injection was kept constant (1 mL/min) during each treatment. All animals were carefully observed for an additional 4 weeks, with necessary food and water supply. Various parameters were measured and compared with the values obtained prior to treatment. All animals were then euthanized and various parameters determined after 4 weeks.

Body general parameters

All animals were weighed once every week. The objective signs, including cleanliness, behavior, and food intake were recorded every day.

Blood analysis

Blood samples were collected from the veins of the animals before administration and every week up to 4 weeks after treatment. The pertinent blood indices were determined with routine methods and an autoanalyzer.[18]

Autopsy study

Four weeks after administration, all animals were sacrificed by exsanguination and dissection. During the process of dissecting, the parenchymatous organs' color, texture, and lumps were carefully examined. In the meantime, the weight of the heart, liver, spleen, lung, kidney, and brain were measured and recorded. The organ–body index was calculated according to the following formula:[19]

$$\text{Organ–body weight index (\%)} = \text{Wet organ weight/Body weight} \times 100\% \quad (3)$$

Histopathological study

Small organ pieces (3–5 mm thick) were fixed in 10% formal-saline (0.9% saline in 10% formaldehyde) for 24 hours and washed in running water for another 24 hours. Samples were dehydrated by passing through 50%, 70%, 90%, and 100% alcohol over a 2-day period, and then cleared in benzene to remove alcohol until the tissues became transparent. This was followed by staining with hematoxylin-eosin and thorough examination using a light microscope.[20,21]

Statistical analysis

Data were analyzed using SPSS Statistics (v 11.5; IBM Corporation, Somers, NY) software. The statistical significance of differences in mean values between the groups was analyzed using one-way analysis of variance. *P*-values <0.05 were considered statistically significant.

Results

Characterization of Fe_3O_4@Au composite MNPs

The self-prepared Fe_3O_4@Au composite MNPs were approximately spherical, high electron-dense, and uniform in size as observed by TEM and SEM (Figure 1A and B). Meanwhile, EDS confirmed that the prepared nanoparticles contained the elements of Fe, Au, and O (Figure 1B inset). The average diameter detected by Malvern laser particle size analyzer was about 35 nm, with a narrow diameter distribution for Fe_3O_4@Au composite MNPs (Figure 1C) and about 20 nm for Fe_3O_4-MNPs (Figure 1C inset). And the zeta potential of Fe_3O_4@Au composite MNPs at pH 7.4 was -23.2 ± 1.8 mV (Figure 1D) compared with the zeta potential value of -3.6 ± 1.8 mV for Fe_3O_4-MNPs (Figure 1D inset). Moreover, the UV-vis absorption spectra of Fe_3O_4@Au composite MNPs indicated 612 nm of the absorption peak (Figure 1E, curve b), while the Fe_3O_4-MNPs absorption spectra were increased with the wavelength decrease in the range 900–300 nm

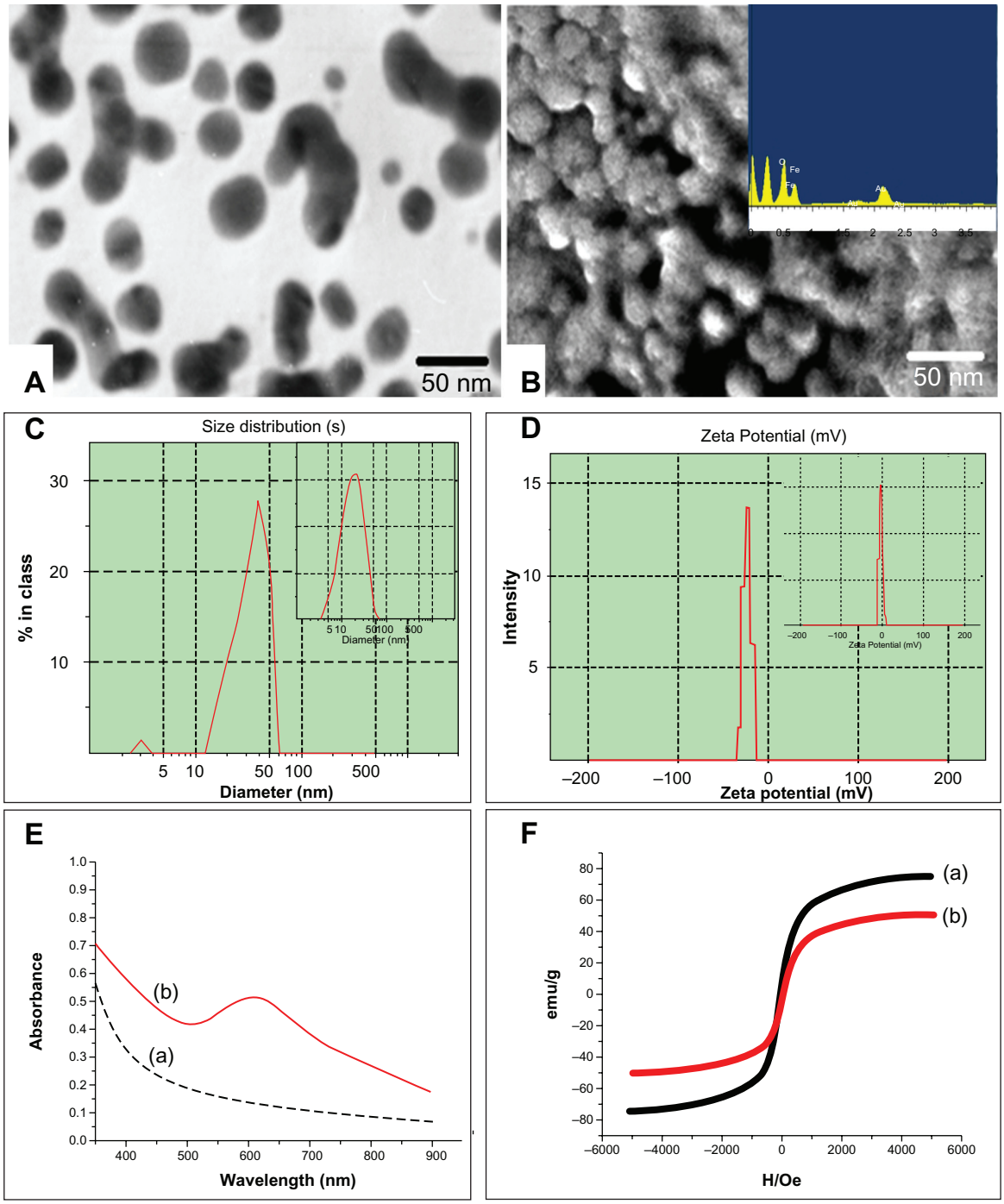

Figure 1 Characterization of Fe_3O_4@Au composite MNPs. (**A**) Transmission electron microscopy image; (**B**) scanning electron microscopy image and energy dispersive spectrometry (inset); (**C**) the average diameter of Fe_3O_4@Au composite MNPs and Fe_3O_4-MNPs (inset); (**D**) the zeta potential of Fe_3O_4@Au composite MNPs and Fe_3O_4-MNPs (inset); (**E**) ultraviolet-visible absorption spectra of Fe_3O_4@Au composite MNPs (curve b) and Fe_3O_4-MNPs (curve a); and (**F**) hysteresis loops of Fe_3O_4@Au composite MNPs (curve b) and Fe_3O_4-MNPs (curve a).

Abbreviation: MNPs, magnetic nanoparticles.

(Figure 1E, curve a). The magnetic hysteresis loops measured at 300 K showed that the saturation magnetization (M_s) value of Fe_3O_4-MNPs was 75.5 emu/g (Figure 1F, curve a), while the value of Fe_3O_4@Au MNPs was 51.8 emu/g (Figure 1F, curve b).

The cytotoxicity of Fe_3O_4@Au composite MNPs

The morphological changes of L929 cells after treatment with different concentrations of Fe_3O_4@Au composite MNPs leaching liquor were observed by inverted microscopy.

As shown in Figure 2B–E, the shapes and growth of the treated cells were similar to those of cells in the negative group (Figure 2A). They exhibited normal features, such as clear edges, homogeneous staining, and no cell fragments, while the cells of the positive group became small and globular, and even parts of cells were suspended 48 hours later (Figure 2F). Only small amounts of cells survived. The results of the MTT assay are shown in Figure 3. According to RGR and toxicity grade conversion table (see Table 1), the toxicity of Fe_3O_4@Au composite MNPs leaching liquor was classified as grade 1, which is safe to the cells. This was in agreement with the findings from inverted microscopy and demonstrated that Fe_3O_4@Au composite MNPs did not show cytotoxicity in vitro.

Hemolysis experimental results of Fe_3O_4@Au composite MNPs

The hemolysis rates at 545 nm are listed in Table 2 for each experimental group. Hemolysis rates at the different concentrations of Fe_3O_4@Au composite MNPs were 0.278%, 0.232%, and 0.197%, respectively, far less than 5%, which is the threshold for a hemolytic reaction.[14]

MN results of Fe_3O_4@Au composite MNPs

In this study, the MN formation rates of 5.00, 3.75, 2.50, and 1.25 g/kg experimental groups, negative control group, and positive control group were 2.5‰, 2.7‰, 2.6‰, 2.3‰, 2.1‰, and 26.2‰ respectively (Figure 4), showing a significant difference between the experimental groups and the positive control group ($P < 0.05$). But MN formation rates at different doses of experimental groups showed no statistical difference compared with the negative control group ($P > 0.05$).

Acute toxicity in mice

Some behavioral changes such as crouching, sluggishness, bradypnea, and slow response to external stimuli were observed among some animals immediately after Fe_3O_4@Au composite MNP administration. However, some resumed normal activity about 2 hours after the treatment. Interestingly, Fe_3O_4@Au composite MNP administration of 1.77 g/kg did not bring any notable changes to the animals. The deaths of most mice occurred during the first day after administration (Table 3). Mortality rates in the treatment groups were used to calculate the LD_{50} of Fe_3O_4@Au composite MNPs, which evaluate short-term toxicity after intraperitoneal administration. The LD_{50} of the material to the mice was 8.39 g/kg, and its 95% confidence interval (CI) was 6.58–10.72 g/kg from the acute toxicological study.

Acute toxicity in beagle dogs

Effect of Fe_3O_4@Au composite MNPs on the general behavior

The acute general toxicity test was used to evaluate short-term toxicity after liver administration. Behavioral changes including slobbering, astasia, instability of gait, convulsion, anepithymia, and respiratory depression were not observed among animals in the experimental group. Both control group and experimental group animals displayed normal physical behavior during the 4-week observation period. All animals were weighed once a week. There was

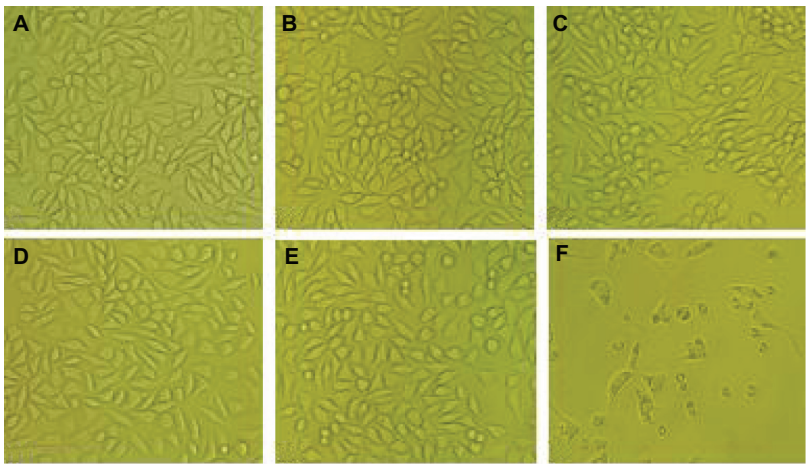

Figure 2 Morphology analysis of L929 cells incubated at different concentrations of Fe_3O_4@Au composite magnetic nanoparticles leaching liquor. (**A**) Negative control; (**B**) 25% leaching liquor; (**C**) 50% leaching liquor; (**D**) 75% leaching liquor; (**E**) 100% leaching liquor; and (**F**) positive control.
Note: Inverted microscopy, ×100 magnification.

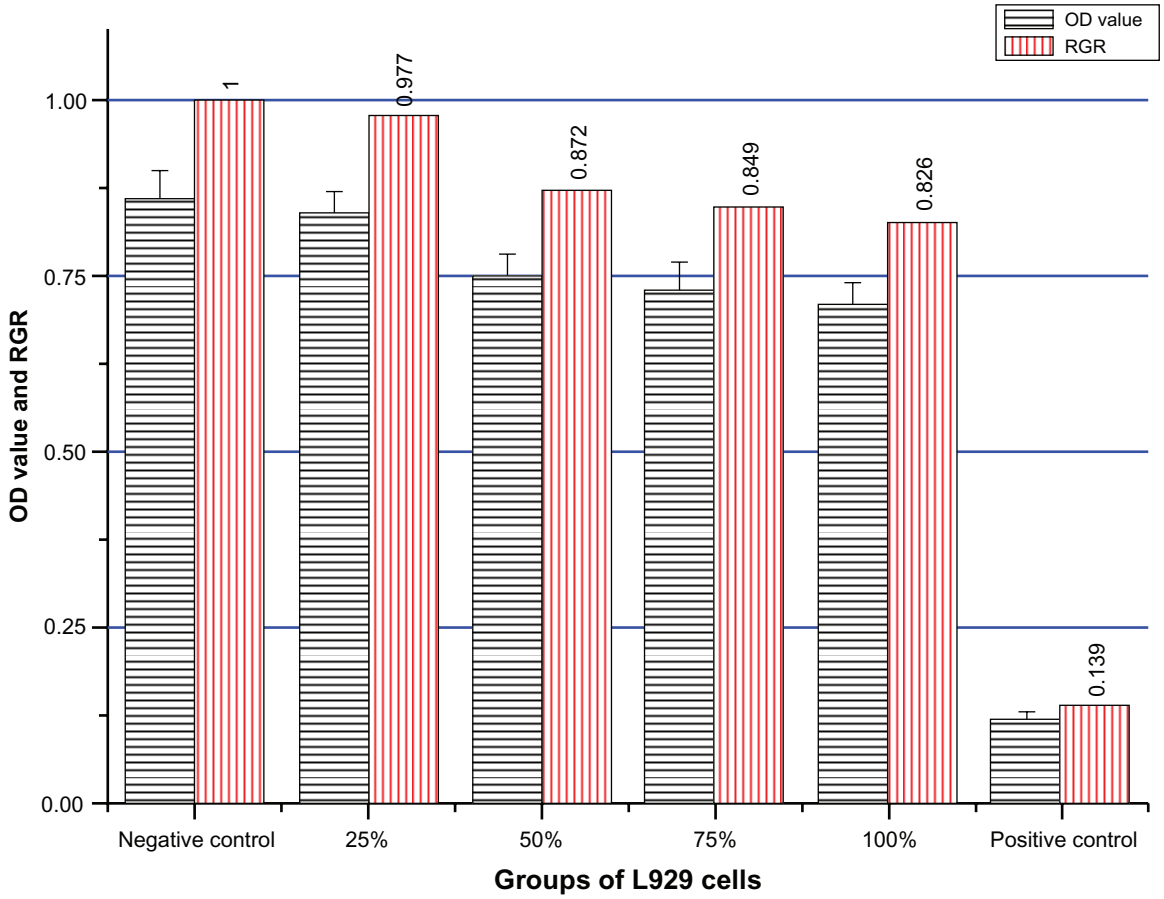

Figure 3 The MTT results of Fe_3O_4@Au composite magnetic nanoparticles.
Notes: n = 8, mean ± standard deviation. The RGR of L929 cells incubated with 25%, 50%, 75%, and 100% leaching liquor were 0.977, 0.872, 0.849, and 0.826, respectively, which all classified as toxicity grade 1.
Abbreviations: MTT, 3-(4,5-dimethylthiazol-2-yl)-2,5-diphenyltetrazolium bromide; OD, optical density; RGR, relative growth rate.

no significant difference in body weight values of beagle dogs between the experimental group and the control group ($P > 0.05$; Figure 5).

Effect of Fe_3O_4@Au composite MNPs on the biochemical and hematological parameters

The effect of liver injection of Fe_3O_4@Au composite MNPs on alanine aminotransferase (ALT), aspartic acid aminotransferase (AST), blood urea nitrogen (BUN), and creatinine (Cr) are presented in Figures 6 and 7, showing no significant differences between the experimental group and the control group in the data of ALT, AST, BUN, and Cr during the 4 weeks ($P > 0.05$). Furthermore, no significant differences were observed for hematological parameters between the experimental group and the control group ($P > 0.05$; detailed data can be seen in Table S1).

Table 2 Hemolysis test of Fe_3O_4@Au composite magnetic nanoparticles

Groups	OD	HR (%)
Negative control	0.0143 ± 0.002	–
100 mg/mL Fe_3O_4@Au	0.0167 ± 0.003	0.278
75 mg/mL Fe_3O_4@Au	0.0163 ± 0.001	0.232
50 mg/mL Fe_3O_4@Au	0.0160 ± 0.004	0.197
Positive control	0.8762 ± 0.012	–

Note: n = 3, mean ± standard deviation.
Abbreviations: OD, optical density; HR, hemolysis rate.

Effect of Fe_3O_4@Au composite MNPs on the organs

The autopsy study was carried out 4 weeks after the animals were treated with Fe_3O_4@Au composite MNPs. The organs, including heart, liver, spleen, lung, kidney, brain, adrenal glands, and pancreas, were carefully examined and investigated. No noticeable pathological changes such as swelling, shrinking, nodules, collapse, hard texture, and thickened capsule could be observed by the naked eye. No significant differences in organ weight or organ–body weight indices were found between the experimental group and the control group ($P > 0.05$; Figure 8).

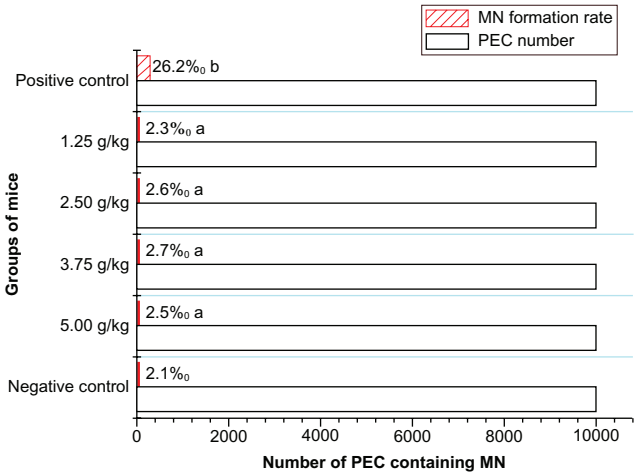

Figure 4 The results of MN test of Fe_3O_4@Au composite magnetic nanoparticles.
Notes: n = 10. [a]$P > 0.05$, MN formation rates of Fe_3O_4@Au groups compared with negative control; [b]$P < 0.05$, MN formation rates between Fe_3O_4@Au groups and positive control.
Abbreviations: MN, micronucleus; PEC, polychromatic erythrocytes.

Effect of Fe_3O_4@Au composite MNPs on histopathological changes

Histopathological investigation was performed after the autopsy study. From the histological sections (Figure 9A), no significant pathological changes were detected in the liver tissue of experimental dogs, except for lots of Fe_3O_4@Au composite MNPs taken up by cells around the needle passage and a small area of mechanical damage. Other organs including heart, spleen, lung, kidney, and brain showed no sign of pathological changes such as edema, atrophy, steatosis, liquefaction necrosis, hyalinization, calcification, and hemosiderosis compared with the corresponding organs from the dogs in the control group (Figure 9B–F).

Discussion

Recently, the unique structure and magnetic-optical properties of Fe_3O_4@Au composite MNPs have made them promising materials for a wide range of biological applications such as cell labeling, tracking, imaging, gene delivering, and sensing. Particularly, there are potential applications in the intracellular/interstitial MFH and NIR hyperthermia.[22–25] However, there is concern about the potential toxicological effects of them in vitro and in vivo. At present, it is widely recognized that Fe_3O_4-MNPs are metabolized, stored, and transported through human tissues by proteins including ferritin, transferritin, hemosiderin, and others, such that the resultant iron is incorporated into the iron pool. Many researchers have synthesized Fe_3O_4-MNPs successfully with satisfactory biocompatibility and explored their biomedical applications.[26–28] On the other hand, some researchers reported that bare Fe_3O_4-MNPs induced the formation of free hydroxyl radical species that reacted with intracellular constituents such as the cell's endogenous DNA, thus inhibiting cellular function and proliferation.[29,30] Moreover, it was found that exposure to dextran- or citric acid-coated Fe_3O_4-MNPs, of an approximate size of 31–38 nm, resulted in a dose-dependent decrease of HUVEC viability in vitro.[31] These results confirm that the toxicity of Fe_3O_4-MNPs affect the biocompatibility and biosafety in vitro. Meanwhile, it was reported that the gold shell coating on the Fe_3O_4-MNPs surface improved the biocompatibility for cellular application, particularly at high magnetite loading. The improved biocompatibility may be attributed to the presence of gold shells which prevents the leaching of iron in acidic intracellular degradation process.[32] Similarly, the protective properties of the gold coating have also been reported by others.[33] However, the literature also reported conflicting data regarding the cytotoxicity of

Table 3 The results of acute toxicity testing of Fe_3O_4@Au composite MNPs

Group	Dosage		n	Death number	Death rate (p)	Survival rate (q)	p × q
	$g \cdot kg^{-1}$	Logarithm					
1	1.77	0.249	10	0	0	1.0	0
2	2.51	0.399	10	0	0	1.0	0
3	3.54	0.549	10	2	0.2	0.8	0.16
4	5.00	0.699	10	2	0.2	0.8	0.16
5	7.06	0.849	10	4	0.4	0.6	0.24
6	9.98	0.999	10	5	0.5	0.5	0.25
7	14.09	1.149	10	7	0.7	0.3	0.21
8	19.89	1.299	10	10	1.0	0	0
		i = 0.15			$\sum p = 3.0$		

Notes: $\lg LD_{50} = X_k - I(\sum p - 0.5) = 1.299 - 0.15\ (3.0 - 0.5) = 0.924$; $s_m = i \times (\sum pq/n)^{1/2} = 0.15 \times 0.36 = 0.054$; $\lg LD_{50}$ and its 95% CI were $0.924 \pm 1.96 \times 0.054 = 0.924 \pm 0.106$; LD_{50} and its 95% CI were 8.39 g/kg (6.58–10.72 g/kg).
Abbreviations: LD_{50}, median lethal dose; MNPs, magnetic nanoparticles.

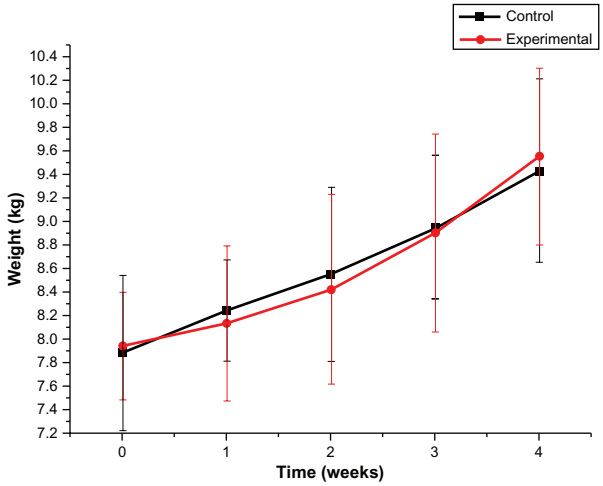

Figure 5 Effect of Fe_3O_4@Au composite MNPs administered via liver injection on body weight (kg) in beagle dogs.
Notes: n = 6, mean ± standard deviation. There was no significant difference in body weight values of beagle dogs between the experimental group and the control group at the five time points of before administration and 1, 2, 3, and 4 weeks after administration of Fe_3O_4@Au composite MNPs ($P > 0.05$).
Abbreviation: MNPs, magnetic nanoparticles.

gold nanoparticles in vitro. For example, some researchers demonstrated that different sized gold nanoparticles with varying surface chemistries were not toxic to human cells.[34] But others reported that gold nanoparticles demonstrated a size-dependent toxicity for sizes ranging from 0.8–15 nm.[35] Moreover, it was discovered that the electrical charge of the nanoparticle played a key role in determining toxicity, with cationic gold nanoparticles displaying moderate toxicity, while their anionic counterparts exhibited no toxic effects.[36] Interestingly, Alkilany et al reported that gold nanoparticles bore the same effective charge in the biological media because serum proteins adsorbed to gold nanoparticles, regardless of the initial surface charge, suggesting that physiochemical surface properties of nanomaterials change substantially after coming into contact with biological media. Such changes should be taken into consideration when examining the biological properties or environmental impact of nanoparticles.[37] Based on these results, it is imperative to systematically evaluate the biocompatibility of Fe_3O_4@Au

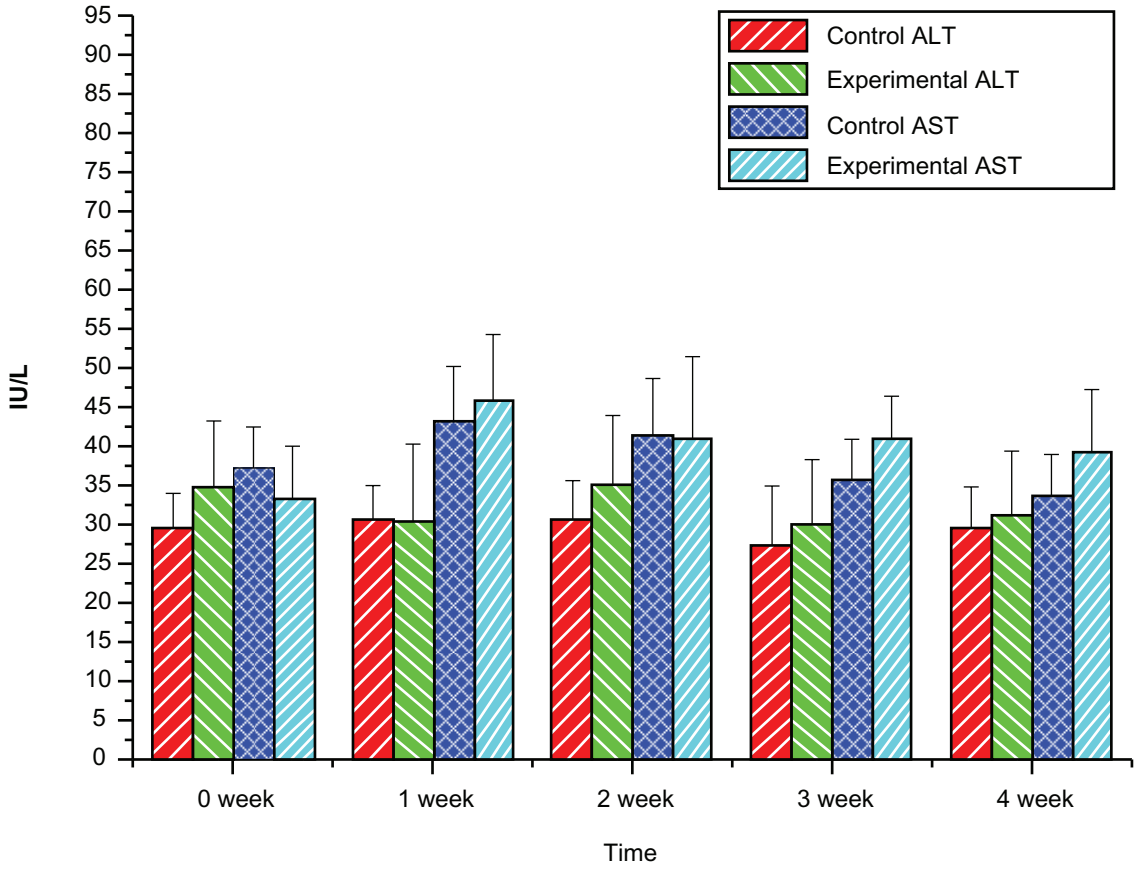

Figure 6 Liver function of beagle dogs in 4-week toxicity study of Fe_3O_4@Au composite MNPs.
Notes: n = 6, mean ± standard deviation. ALT and AST of the experimental group administered with Fe_3O_4@Au composite MNPs showed no significant difference compared with the control group ($P > 0.05$).
Abbreviations: MNPs, magnetic nanoparticles; ALT, alanine aminotransferase; AST, aspartic acid aminotransferase.

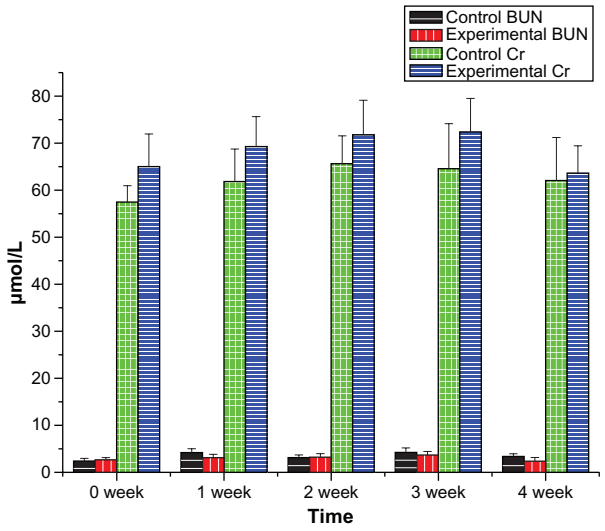

Figure 7 Renal function of beagle dogs in 4-week toxicity study of Fe_3O_4@Au composite MNPs.
Notes: n = 6, mean ± standard deviation. BUN and Cr of the experimental group administered with Fe_3O_4@Au composite MNPs showed no significant difference compared with the control group ($P > 0.05$).
Abbreviations: MNPs, magnetic nanoparticles; BUN, blood urea nitrogen; Cr, creatinine.

composite MNPs and their toxicity within biological systems, especially in vivo, since results from in-vitro and in-vivo testing may be quite different.

A previous study reported the synthesis strategy involving a hetero-interparticle coalescence of molecularly capped Au nanoparticles (2 nm) and iron-oxide nanoparticles (30–50 nm) as precursors in mixed solution, leading to core–shell nanoparticles. The results showed

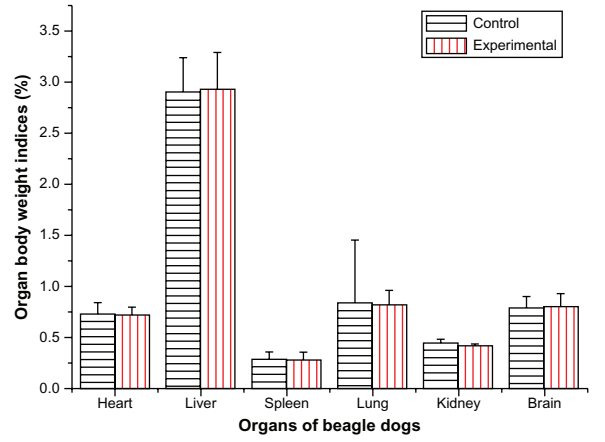

Figure 8 Effect of Fe_3O_4@Au composite magnetic nanoparticles administered via liver injection on organ body weight indices of beagle dogs after 4 weeks.
Notes: n = 6, mean ± standard deviation. There was no significant difference in organ body weight indices including heart, liver, spleen, lung, kidney, and brain between the experimental group and the control group ($P > 0.05$).

that gold shell-coated Fe_3O_4-MNPs existed as aggregates with a broad size distribution, and the longest aggregate dimension varied from 100 nm to 2 μm. However, they exhibited improved biocompatibility in mammalian cells.[32] The strategy used in this present study involves sequential formation of the iron-oxide core and gold shell, and the composite particles were prepared by the reduction of Au^{3+} with hydroxylamine in the presence of Fe_3O_4-MNPs, with the average diameter of 20 nm as seeds. Compared with other reports,[3,32] the Fe_3O_4@Au composite MNPs in this present study were proved to retain the quasi-spherical shape and uniform size by TEM and SEM. The results of laser particle size analysis illustrated that the average diameter of Fe_3O_4-MNPs was about 20 nm. After modification of the Fe_3O_4-MNPs with gold shell, the average diameter of the resulting core–shell Fe_3O_4@Au composite MNPs was about 35 nm, with a narrow diameter distribution. Thus, the thickness of the gold shell was estimated to be 7–8 nm. However, proper shell thickness is essential to obtain new optical properties and retain enough magnetism characteristics for Fe_3O_4@Au composite MNPs. UV-vis spectra were therefore obtained to investigate the preparation and the optical properties of the self-prepared Fe_3O_4@Au composite MNPs. The UV-vis absorption spectra showed that Fe_3O_4-MNP absorption spectra had no dramatic absorption in the visible region. However, after the Fe_3O_4-MNPs were coated with gold shell, 612 nm of the absorption peak was remarkably observed owing to the surface plasmon, indicating that the gold shell layer was formed on the surface of the Fe_3O_4 core, consistent with the observation from other reports.[3,4] In contrast to the literature, the Fe_3O_4@Au composite MNPs in this present study had broader absorption spectra and redshifted maximum absorption wavelength.[3,38,39] Such a redshift phenomenon of the plasmon absorption can be understood in terms of plasmon hybridization with the gold shell layer growth. In addition, because the gold shell layer outside the Fe_3O_4 core forms a rough surface after a coating of three iterations, strong interaction and coupling of the surface plasmon exists between neighboring nanoparticles, which may also contribute to the plasmon resonance redshift.[40]

Furthermore, the magnetic measurement showed that the Fe_3O_4@Au composite MNPs in this present study retained superparamagnetic properties with low coercivity and high M_s at room temperature, similar to Fe_3O_4-MNPs used in MFH.[9] The M_s values of Fe_3O_4-MNPs and Fe_3O_4@Au composite MNPs were estimated to be 75.5 and 51.8 emu/g,

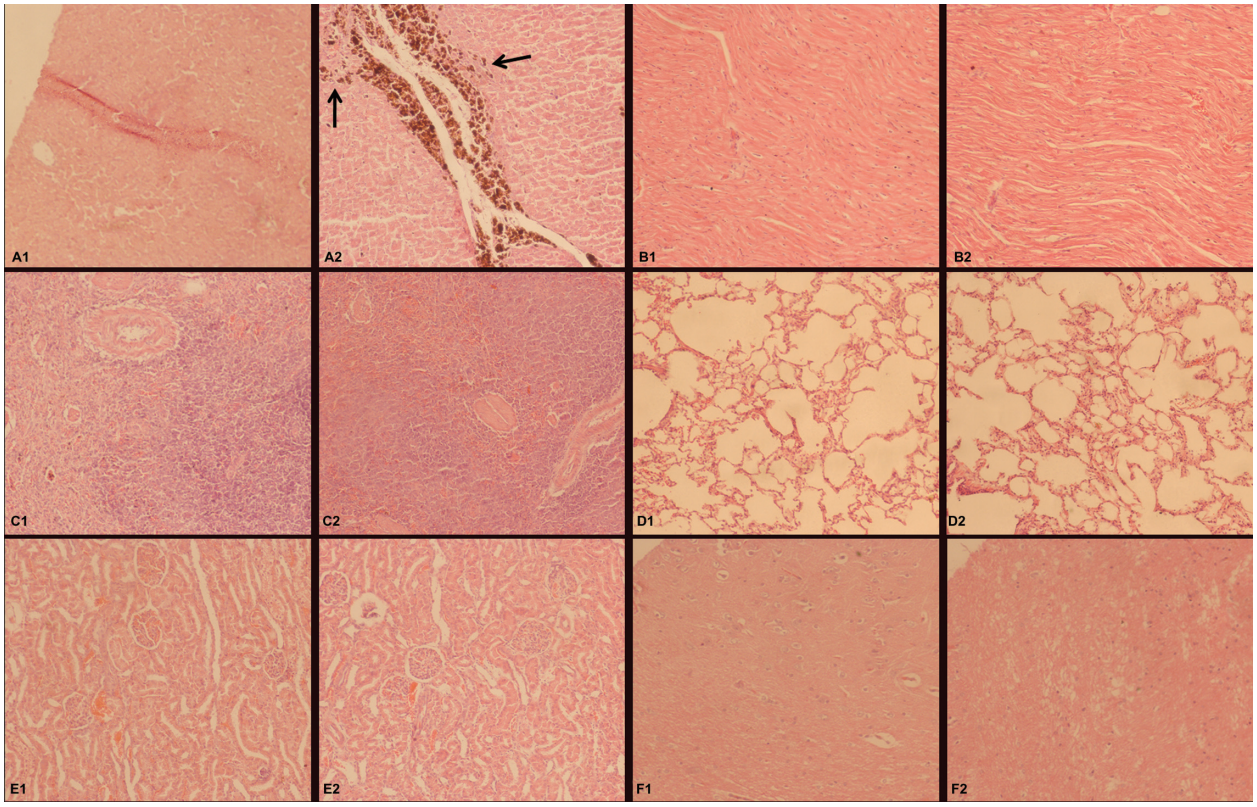

Figure 9 Effect of Fe_3O_4@Au composite MNPs administered via liver injection on the tissue of beagle dogs after 4 weeks (hematoxylin-eosin staining, ×100 magnification). (**A1**) Little impact on the liver of the control group; (**A2**) Fe_3O_4@Au composite MNPs were taken up by cells around the needle passage in the liver of the experimental group, indicated by arrows; (**B**–**F**) no significant pathological changes were detected in the tissues including heart (**B1** and **B2**), spleen (**C1** and **C2**), lung (**D1** and **D2**), kidney (**E1** and **E2**), and brain (**F1** and **F2**).
Abbreviation: MNPs, magnetic nanoparticles.

respectively, which are much lower than that of bulk Fe_3O_4 (M_s = 84 emu/g). Generally, the M_s decreased significantly when the gold shell formed on the surface of Fe_3O_4 MNPs. This reduction is expected as the surface magnetic order can be affected by structural distortions that cause spin canting.[41] However, the M_s of Fe_3O_4@Au composite MNPs is higher than that from other research.[39,40] In addition, the detection of effective surface charge showed that the zeta potential of Fe_3O_4-MNPs was close to neutral charge (–3.6 ± 1.8 mV) at pH 7.4, the presence of gold shell shifted the zeta potential value to –23.2 ± 1.8 mV. A slightly high negative zeta potential imparted by Fe_3O_4@Au composite MNPs compared with Fe_3O_4-MNPs confirms an amount of gold coverage on the magnetite surface, which was in agreement with the literature.[32]

Next in this present study, the toxicity of self-prepared Fe_3O_4@Au composite MNPs was investigated through MTT assay, hemolysis test, MN assay, and acute toxicity testing in rodent and Canidae animals. The MTT assay is very often used to evaluate cell proliferation and the viability for biomaterial toxicity.[13] In this present experiment, Fe_3O_4@Au composite MNPs with various concentrations of leaching liquor (100%, 75%, 50%, and 25%) were adjusted to test the cytotoxicity on L929 cells. The morphological observations showed that no significant toxic effects were seen compared with the negative control under the microscope, indicating that Fe_3O_4@Au composite MNPs have a minimal impact on the cell population as the cells remained viable and continued to proliferate. The toxicity of Fe_3O_4@Au composite MNPs was classified as grade 1, suggesting that they have good biocompatibility for cellular application, consistent with the literature, which reported negligible impact of Fe_3O_4@Au with amine functional group on mammalian cells.[42]

The hemolysis test is mainly used to evaluate the hemocompatibility of materials by detecting hemolyzation of erythrocytes. The erythrocyte membrane integrity may be destroyed by both mechanical injury of the particle surface and the chemical action of soluble remnant molecules, resulting in hemolyzation when Fe_3O_4@Au composite MNPs

are used for thermotherapy. So the extent of hemolysis could be calculated by detecting the absorbance of released free hemoglobin using ultraviolet spectrophotometry.[43,44] In this study, hemolysis rates at different concentrations of Fe_3O_4@Au composite MNPs were all far less than 5%, which is the threshold for a hemolytic reaction, indicating that Fe_3O_4@Au composite MNPs do not cause hemolysis and have good hemocompatibility, which is in agreement with previous studies.[11,16]

The short-term genetic toxicity was tested by MN assay, which is a rapid detection method of chromosome damage and interference with cell mitosis caused by the biological materials. If the result of this test is negative, it isn't necessary to perform the carcinogenic test.[45] Previously, Wu et al adopted the dosages of 5.00–1.25 g/kg to assess the short-term genetic toxicity of self-assembled Fe_3O_4-MNPs loaded with daunorubicin (DNR).[16] In this study, the MN formation rates of experimental groups with different dosages from 5.00 to 1.25 g/kg showed no statistical difference compared with the negative control group, but a significant difference compared with the positive control group, suggesting Fe_3O_4@Au composite MNPs have no inherent toxicity to bone-marrow cells in mice. The results are similar to the MN assay of Fe_3O_4-MNPs and Fe_3O_4-MNPs loaded with DNR.[11,16] Thus, it can be inferred that these nanoparticles do not induce cacogenesis or mutations.

The acute toxicity testing was used to evaluate short-term toxicity after intraperitoneal administration in mice. In tumor thermotherapy, it is crucial to optimize dosing not only for effectively heating tumor tissue or promoting apoptosis of tumor cells, but also for reducing the systemic side effects. The LD_{50} of Fe_3O_4@Au composite MNPs administered by intraperitoneal injection was determined to be 8.39 g/kg in mice, and its 95% CI was found to fall in the range of 6.58–10.72 g/kg from the acute toxicological study. In contrast to Fe_3O_4-MNPs with the LD_{50} arriving at 7.57 g/kg and $Mn_{0.5}Zn_{0.5}Fe_2O_4$-MNPs at 7.19 g/kg, Fe_3O_4@Au composite MNPs have a wider safety margin.[11,46] These parameters provide critical guidelines for the administration of this material in future studies.

Previous research of pharmacokinetics and tissue distribution in mice showed that Fe_3O_4-MNPs were mostly taken up in the liver, suggesting the curative effect could be more pronounced for tumors in the liver.[47] But the hepatotoxicity following gold salt therapy also has been previously reported, while accumulation of gold particles around hepatic veins, probably within macrophages, was observed, although no abnormal changes on the hematological parameters were observed.[48] Therefore, investigated in this present paper was whether Fe_3O_4@Au composite MNPs could cause short-term systemic toxic reactions during a 4-week period after liver injection in beagle dogs. The dosage of Fe_3O_4@Au composite MNPs via liver injection was 100 mg/kg, which was also adopted in the acute toxicological observations of Fe_3O_4-MNPs loaded with DNR.[16] Typical toxicological responses such as slobbering, astasia, and anepithymia were not observed. Meanwhile, the body weights of the animals were measured every week, since body weight loss has been used as an indicator of adverse effects of drugs and chemicals.[49] There was no significant difference in body weight of beagle dogs after administration of Fe_3O_4@Au composite MNPs compared with the control group. These results imply that liver injection of Fe_3O_4@Au composite MNPs made a negligible impact on the general behavior of beagle dogs. Moreover, the levels of ALT, AST, BUN, and Cr did not increase significantly when compared with those of the control group, suggesting that Fe_3O_4@Au composite MNPs did not cause both liver and kidney injury.

In addition, no abnormal changes of the hematological parameters were observed compared with the control group, showing that the lymphohemopoietic system was not affected by the Fe_3O_4@Au composite MNPs administered to the beagle dogs. Furthermore, it was demonstrated that Fe_3O_4@Au composite MNPs did not induce lesions of organs and tissues by both autopsy study and histopathological investigation.

Meanwhile, it is noteworthy that Fe_3O_4@Au composite MNPs were almost ingested and deposited in the liver because no nanoparticles and hemosiderosis were observed in other organs including heart, spleen, lung, kidney, and brain, confirming the potential application in the intracellular and interstitial MFH combined with NIR hyperthermia on liver tumors with organ targeting and safety to biological systems in general. Thus, summarizing all the experimental results, it can be assumed that Fe_3O_4@Au composite MNPs do not cause any short-term systemic toxic reactions in beagle dogs with the dosage used in this study. In contrast to the investigation on the biocompatibility of magnetic albumin nanosphere (MAN) in a very recent publication, Fe_3O_4@Au MNPs indicate desirable biocompatibility in vivo at the high concentration of 100 mg/mL when MAN showed good biocompatibility at the concentration of 5 mg/mL in mice.[50]

Conclusion

In conclusion, the results of this study show that Fe_3O_4@Au composite MNPs appear to be highly biocompatible and safe

nanoparticles according to the evaluation of toxicity in vivo and in vitro. Considering that some of the Food and Drug Administration-approved MRI contrast agents are made of Fe_3O_4, Fe_3O_4@Au composite MNPs have a potential to be used as safe optical and thermal agents, allowing the combination of cancer detection and cancer-specific hyperthermic treatment. The results of this study provide experimental foundation for further clinical research and evaluation of this promising material.

Acknowledgments

This work was supported by the Chinese National 863 Plan (No. 2007AA03Z356), the Chinese National Natural Science Foundation (No. 30770584 and No. 81171452), and the Science and Technology Development Foundation of Nanjing Medical University (No. 08NMUZ015).

Disclosure

The authors report no conflicts of interest in this work.

References

1. Jordan A, Scholz R, Wust P, et al. Effects of magnetic fluid hyperthermia (MFH) on C3H mammary carcinoma in vivo. *Int J Hyperthermia*. 1997;13:587–605.
2. O'Neal DP, Hirsch LR, Halas NJ, Payne JD, West JL. Photo-thermal tumor ablation in mice using near infrared-absorbing nanoparticles. *Cancer Lett*. 2004;209:171–176.
3. Wang L, Luo J, Fan Q, et al. Monodispersed core-shell Fe_3O_4@Au nanoparticles. *J Phys Chem B*. 2005;109:21593–21601.
4. Liu HL, Sonn CH, Wu JH, Lee KM, Kim YK. Synthesis of streptavidin-FITC-conjugated core-shell Fe_3O_4-Au nanocrystals and their application for the purification of $CD4^+$ lymphocytes. *Biomaterials*. 2008;29:4003–4011.
5. Jin H, Kang KA. Application of novel metal nanoparticles as optical/thermal agents in optical mammography and hyperthermic treatment for breast cancer. *Adv Exp Med Biol*. 2007;599:45–52.
6. Kouassi GK, Irudayaraj J. Magnetic and gold-coated magnetic nanoparticles as a DNA sensor. *Anal Chem*. 2006;78:3234–3241.
7. Gupta AK, Gupta M. Synthesis and surface engineering of iron oxide nanoparticles for biomedical applications. *Biomaterials*. 2005;26:3995–4021.
8. Yan S, Zhang D, Zheng J, et al. Study on the therapeutic effect of Fe_2O_3 nanometer magnetic fluid hyperthermia on liver cancer. *China Journal of Experimental Surgery*. 2004;21:1443–1446.
9. Du Y, Zhang D, Liu H, Lai R. Thermochemotherapy effect of nanosized As_2O_3/Fe_3O_4 complex on experimental mouse tumors and its influence on the expression of CD44v6, VEGF-C and MMP-9. *BMC Biotechnol*. 2009;9:84.
10. Kirkpatrick CJ, Bittinger F, Wagner M, et al. Current trends in biocompatibility testing. *Proc Inst Mech Eng H*. 1998;212:75–84.
11. Du Y, Zhang D, Ni H, et al. The biocompatibility of Fe_3O_4 magnetic nanoparticles used in tumor hyperthermia. *Journal of Nanjing University (Natural Science)*. 2006;42:324–330.
12. Yan S, Zhang D, Gu N, et al. The biocompatibility study of magnetic nanoparticles containing Fe_2O_3 used in tumor hyperthermia. *J Southeast Univ (Med Sci Edi)*. 2005;24:8–12.
13. Pieters R, Loonen AH, Huismans DR, et al. In vitro drug sensitivity of cells from children with leukemia using the MTT assay with improved culture conditions. *Blood*. 1990;76:2327–2336.
14. Sun J, Gu GZ, Qian YF. Influence of different contact ways and extracting conditions on the hemolytic effect of biomaterials. *J Biomed Eng*. 2003;20:8–10.
15. Zhang WY, Shen Y, Li N, et al. Evaluation of biocompatibility of fiber-reinforced dental composites. *Med J Chin PLA*. 2004;29:345–347.
16. Wu W, Chen B, Cheng J, et al. Biocompatibility of Fe_3O_4/DNR magnetic nanoparticles in the treatment of hematologic malignancies. *Int J Nanomedicine*. 2010;5:1079–1084.
17. Twaij HA, Kery A, Al-Khazraji NK. Some pharmacological, toxicological and phytochemical investigations on *Centaurea phyllocephala*. *J Ethnopharmacol*. 1983;9:299–314.
18. Lott JA. Practical problems in clinical enzymology. *CRC Crit Rev Clin Lab Sci*. 1977;8:277–301.
19. Guo Q, Qi Q, You Q, Gu H, Zhao L, Wu Z. Toxicological studies of gambogic acid and its potential targets in experimental animals. *Basic Clin Pharmacol Toxicol*. 2006;99:178–184.
20. Akdogan M, Kilinç I, Oncu M, Karaoz E, Delibas N. Investigation of biochemical and histopathological effects of Mentha piperita L. and Mentha spicata L. on kidney tissue in rats. *Hum Exp Toxicol*. 2003;22:213–219.
21. Abd-Elhamid HF. Investigation of induced biochemical and histopathological parameters of acetonitril extract of Jatropha carcus in albino rats. *J Egypt Soc Parasitol*. 2004;34:397–406.
22. Qiu JD, Xiong M, Liang RP, Peng HP, Liu F. Synthesis and characterization of ferrocene modified Fe_3O_4@Au magnetic nanoparticles and its application. *Biosens Bioelectron*. 2009;24:2649–2653.
23. Barry SE. Challenges in the development of magnetic particles for therapeutic applications. *Int J Hyperthermia*. 2008;24:451–466.
24. Hirsch LR, Stafford RJ, Bankson JA, et al. Nanoshell-mediated near-infrared thermal therapy of tumors under magnetic resonance guidance. *Proc Natl Acad Sci U S A*. 2003;100:13549–13554.
25. Song HM, Wei Q, Ong QK, Wei A. Plasmon-resonant nanoparticles and nanostars with magnetic cores: synthesis and magnetomotive imaging. *ACS Nano*. 2010;4:5163–5173.
26. Dave SR, Gao X. Monodisperse magnetic nanoparticles for biodetection, imaging, and drug delivery: a versatile and evolving technology. *Wiley Interdiscip Rev Nanomed Nanobiotechnol*. 2009;1:583–609.
27. Sun J, Zhou S, Hou P, et al. Synthesis and characterization of biocompatible Fe_3O_4 nanoparticles. *J Biomed Mater Res A*. 2007;80:333–341.
28. Cheng FY, Su CH, Yang YS, et al. Characterization of aqueous dispersions of Fe(3)O(4) nanoparticles and their biomedical applications. *Biomaterials*. 2005;26:729–738.
29. Emerit J, Beaumont C, Trivin F. Iron metabolism, free radicals, and oxidative injury. *Biomed Pharmacother*. 2001;55:333–339.
30. van den Bos EJ, Wagner A, Mahrholdt H, et al. Improved efficacy of stem cell labeling for magnetic resonance imaging studies by the use of cationic liposomes. *Cell Transplant*. 2003;12:743–756.
31. Wu X, Tan Y, Mao H, Zhang M. Toxic effects of iron oxide nanoparticles on human umbilical vein endothelial cells. *Int J Nanomedicine*. 2010;5:385–399.
32. Arsianti M, Lim M, Lou SN, Goon IY, Marquis CP, Amal R. Bi-functional gold-coated magnetite composites with improved biocompatibility. *J Colloid Interface Sci*. 2011;354:536–545.
33. Ow Sullivan MM, Green JJ, Przybycien TM. Development of a novel gene delivery scaffold utilizing colloidal gold-polyethylenimine conjugates for DNA condensation. *Gene Ther*. 2003;10:1882–1890.
34. Connor EE, Mwamuka J, Gole A, Murphy CJ, Wyatt MD. Gold nanoparticles are taken up by human cells but do not cause acute cytotoxicity. *Small*. 2005;1:325–327.
35. Pan Y, Neuss S, Leifert A, et al. Size-dependent cytotoxicity of gold nanoparticles. *Small*. 2007;3:1941–1949.
36. Goodman CM, McCusker CD, Yilmaz T, Rotello VM. Toxicity of gold nanoparticles functionalized with cationic and anionic side chains. *Bioconjug Chem*. 2004;15:897–900.
37. Alkilany AM, Nagaria PK, Hexel CR, Shaw TJ, Murphy CJ, Wyatt MD. Cellular uptake and cytotoxicity of gold nanorods: molecular origin of cytotoxicity and surface effects. *Small*. 2009;5:701–708.

38. Cui Y, Wang Y, Hui W, Zhang Z, Xin X, Chen C. The synthesis of Gold-Mag nano-particles and their application for antibody immobilization. *Biomed Microdevices*. 2005;7:153–156.
39. Zhou X, Xu W, Wang Y, et al. Fabrication of cluster/shell Fe_3O_4/Au nanoparticles and application in protein detection via a SERS method. *J Phys Chem C*. 2010;114:19607–19613.
40. Levin CS, Hofmann C, Ali TA, et al. Magnetic-plasmonic core-shell nanoparticles. *ACS Nano*. 2009;3:1379–1388.
41. Pal S, Morales M, Mukherjee P, Srikanth H. Synthesis and magnetic properties of gold coated iron oxide nanoparticles. *J Appl Phys*. 2009;7:07B504-07B504-503.
42. Wang FH, Kim DK, Yoshitake T, et al. Diffusion and clearance of superparamagnetic iron oxide nanoparticles infused into the rat striatum studied by MRI and histochemical techniques. *Nanotechnology*. 2011;22:015103.
43. Xi TF. Biological evaluation of biology based on medical devices. *China Medical Device Information*. 1999;5:9–14.
44. Liu WW, Wang T, Zhan DS. Haemolysis test for evaluating the Biocompatibility of SiC implant materials. *CRTER*. 2008;12:1873–1875.
45. Zhao XW, Lin JH, Wang ZR. Study on biocompatibility and security of homemade calcium phosphate cement. *J Fujian Med University*. 2002;36:388–392.
46. Liu J, Zhang J, Wang L, Li Y, Zhang D. Biocompatibility study of $Mn_{0.5}Zn_{0.5}Fe_2O_4$ magnetic nanoparticles. *Key Eng Mater*. 2011;483:552–558.
47. Wang J, Chen Y, Chen B, et al. Pharmacokinetic parameters and tissue distribution of magnetic Fe(3)O(4) nanoparticles in mice. *Int J Nanomedicine*. 2010;5:861–866.
48. Basset C, Vadrot J, Denis J, Poupon J, Zafrani ES. Prolonged cholestasis and ductopenia following gold salt therapy. *Liver Int*. 2010;23:89–93.
49. Tofovic SP, Jackson EK. Effects of long-term caffeine consumption on renal function in spontaneously hypertensive heart failure prone rats. *J Cardiovasc Pharmacol*. 1999;33:360–366.
50. Estevanato L, Cintra D, Baldini N, et al. Preliminary biocompatibility investigation of magnetic albumin nanosphere designed as a potential versatile drug delivery system. *Int J Nanomedicine*. 2011;6:1709–1717.

Supplementary data

Table S1 Hematological values of beagle dogs in 4-week toxicity study of Fe_3O_4@Au composite MNPs

Group/parameter (units)	WBC ($\times 10^9$/L)	RBC ($\times 10^{12}$/L)	Hb (mg/mL)	PLT ($\times 10^9$/L)	Neu ($\times 10^9$/L)	Lymp ($\times 10^9$/L)
Before administration						
Control	11.69 ± 1.80	7.17 ± 0.36	160.17 ± 14.73	298.83 ± 69.34	2.15 ± 1.47	9.00 ± 1.50
Experimental	9.65 ± 2.23	7.23 ± 0.27	168.00 ± 10.24	355.00 ± 103.54	2.35 ± 1.52	7.04 ± 0.83
1 week after administration						
Control	11.45 ± 1.87	7.48 ± 0.44	171.00 ± 19.31	274.50 ± 43.08	2.50 ± 1.53	8.67 ± 0.70
Experimental	11.61 ± 3.56	7.18 ± 0.32	167.67 ± 13.85	307.17 ± 88.05	2.38 ± 0.82	9.31 ± 3.11
2 weeks after administration						
Control	13.46 ± 2.04	7.52 ± 0.65	170.00 ± 21.82	240.67 ± 27.96	2.76 ± 2.03	10.06 ± 3.07
Experimental	12.01 ± 2.50	7.52 ± 0.45	176.67 ± 12.50	340.83 ± 113.71	2.78 ± 1.66	8.66 ± 2.28
3 weeks after administration						
Control	10.88 ± 3.03	7.09 ± 0.86	161.33 ± 28.24	274.00 ± 53.23	2.61 ± 1.19	7.82 ± 2.14
Experimental	14.20 ± 3.13	7.30 ± 0.43	171.67 ± 11.91	291.83 ± 60.71	2.81 ± 1.48	10.99 ± 3.09
4 weeks after administration						
Control	12.76 ± 1.79	7.15 ± 0.38	156.83 ± 19.95	261.67 ± 38.07	3.35 ± 1.55	8.57 ± 0.59
Experimental	11.49 ± 2.04	7.11 ± 0.50	165.17 ± 10.87	322.17 ± 77.87	2.88 ± 1.09	7.95 ± 1.37

Notes: n = 6, mean ± standard deviation. There was no significant difference in hematological values of beagle dogs between the experimental group and the control group at the five time points of before administration and 1, 2, 3, and 4 weeks after administration of Fe_3O_4@Au composite MNPs ($P > 0.05$).

Abbreviations: MNPs, magnetic nanoparticles; WBC, white blood cells; RBC, red blood cells; Hb, hemoglobin concentration; PLT, platelets; Neu, neutrophils; Lymp, lymphocytes.